DALTON
FULL PAPER

Iron(III) and iron(II) complexes of 1-thia-4,7-diazacyclononane ([9]aneN$_2$S) and 1,4-dithia-7-azacyclononane ([9]aneNS$_2$). X-Ray structural analyses, magnetic susceptibility, Mössbauer, EPR and electronic spectroscopy †

Vincent A. Grillo,[a] Lawrence R. Gahan,*[,a] Graeme R. Hanson,[b] Robert Stranger,[c] Trevor W. Hambley,[d] Keith S. Murray,[e] Boujemaa Moubaraki[e] and John D. Cashion[f]

[a] *Department of Chemistry, The University of Queensland, Brisbane, QLD 4072, Australia*
[b] *Centre for Magnetic Resonance, The University of Queensland, Brisbane, QLD 4072, Australia*
[c] *Department of Chemistry, The Australian National University, Canberra, ACT 0200, Australia*
[d] *School of Chemistry, The University of Sydney, Sydney, NSW 2006, Australia*
[e] *Chemistry Department, Monash University, Clayton, Victoria 3168, Australia*
[f] *Physics Department, Monash University, Clayton, Victoria 3168, Australia*

The complexes [Fe([9]aneN$_2$S)$_2$][ClO$_4$]$_2$, [Fe([9]aneN$_2$S)$_2$][ClO$_4$]$_3$ and [Fe([9]aneNS$_2$)$_2$][ClO$_4$]$_2$ ([9]aneN$_2$S = 1-thia-4,7-diazacyclononane and [9]aneNS$_2$ = 1,4-dithia-7-azacyclononane) have been prepared and the latter two characterised by X-ray crystallography. The Mössbauer spectra (isomer shift/mm s^{-1}, quadrupole splitting/mm s^{-1}, 4.2 K) for [Fe([9]aneN$_2$S)$_2$][ClO$_4$]$_2$ (0.52, 0.57), [Fe([9]aneN$_2$S)$_2$][ClO$_4$]$_3$ (0.25, 2.72) and [Fe([9]aneNS$_2$)$_2$][ClO$_4$]$_2$ (0.43, 0.28) are typical for iron(II) and iron(III) complexes. Variable-temperature susceptibility measurements for [Fe([9]aneN$_2$S)$_2$][ClO$_4$]$_2$ (2–300 K) revealed temperature-dependent behaviour in both the solid state [2.95 μ_B (300 K)–0.5 μ_B (4.2 K)] and solution (ΔH^0 20–22 kJ mol^{-1}, ΔS^0 53–60 J mol^{-1} K^{-1}). For [Fe([9]aneN$_2$S)$_2$][ClO$_4$]$_3$ in the solid state [2.3 μ_B (300 K)–1.9 μ_B (4.2 K)] the magnetic data were fit to a simple model ($\mathscr{H} = -\lambda L\cdot S + \mu L_z$) to give the spin–orbit coupling constant (λ) of -260 ± 10 cm^{-1}. The solid-state X-band EPR spectrum of [Fe([9]aneN$_2$S)$_2$][ClO$_4$]$_3$ revealed axial symmetry ($g_\perp = 2.607$, $g_\parallel = 1.599$). Resolution of $g_\perp$ into two components at Q-band frequencies indicated a rhombic distortion. The low-temperature single-crystal absorption spectra of [Fe([9]aneN$_2$S)$_2$][ClO$_4$]$_2$ and [Fe([9]aneNS$_2$)$_2$][ClO$_4$]$_2$ exhibited additional bands which resembled pseudo-tetragonal low-symmetry splitting of the parent octahedral $^1A_{1g} \longrightarrow {}^1T_{2g}$ and $^1A_{1g} \longrightarrow {}^1T_{1g}$ transitions. However, the magnitude of these splittings was too large, requiring $10Dq$ for the thioether donors to be significantly larger than for the amine donors. Instead, these bands were tentatively assigned to weak, low-energy S $\longrightarrow$ Fe^{III} charge-transfer transitions. Above 200 K, thermal occupation of the high-spin $^5T_{2g}$ ground state resulted in observation of the $^5T_{2g} \longrightarrow {}^5E_g$ transition in the crystal spectrum of [Fe([9]aneN$_2$S)$_2$][ClO$_4$]$_2$. From a temperature-dependence study, the separation of the low-spin $^1A_{1g}$ and high-spin $^5T_{2g}$ ground states was approximately 1700 cm^{-1}. The spectrum of the iron(III) complex [Fe([9]aneN$_2$S)$_2$][ClO$_4$]$_3$ is consistent with a low-spin d^5 configuration.

With the ready availability of the ligands 1-thia-4,7-diazacyclononane ([9]aneN$_2$S),[1] 1,4-dithia-7-azacyclononane ([9]aneNS$_2$),[2–4] 1,4,7-triazacyclononane ([9]aneN$_3$)[5] and 1,4,7-trithiacyclononane ([9]aneS$_3$),[6] it is possible to prepare complexes of one metal ion with the series of ligands [9]aneN$_{3-x}$S$_x$ (x = 3–0). Our interest in this area arises from previous observations of the effects of thioether co-ordination on the electrochemical, redox, spectroscopic and magnetic properties of metal complexes such as the macrobicyclic (N$_{6-x}$S$_x$sar) (x = 6, 3, 2, 1 or 0; *e.g.* N$_6$sar = 3,6,10,13,16,19-hexaazabicyclo[6.6.6]icosane) series for cobalt(III)–cobalt(II), chromium(III), nickel(II), copper(II), manganese(II)–manganese(III) and iron(II)[7–16] and the cyclononane ([9]aneN$_{3-x}$S$_x$; x = 3–0) series for nickel(II) and other metal ions.[4,17–19] We have chosen to investigate aspects of the chemistry of iron(II) and iron(III) complexes of the [Fe([9]aneN$_{3-x}$S$_x$)$_2$]$^{n+}$ series. In this paper the synthesis, magnetochemical, EPR and electronic spectroscopy of the complexes [Fe([9]aneNS$_2$)$_2$]$^{2+}$, [Fe([9]aneN$_2$S)$_2$]$^{2+}$ and [Fe([9]aneN$_2$S)$_2$]$^{3+}$ are described, as are the crystal structures for [Fe([9]aneNS$_2$)$_2$]$^{2+}$ and [Fe([9]aneN$_2$S)$_2$]$^{3+}$. The properties of these complexes are compared to those reported elsewhere for [Fe([9]aneN$_3$)$_2$]$^{2+}$ and [Fe([9]aneS$_3$)$_2$]$^{2+}$.

Experimental

The synthetic manipulations leading to the iron(II) complexes were carried out under dry nitrogen using standard Schlenk techniques and a double manifold vacuum line, or in a VAC Vacuum Atmospheres (HE-43-2) controlled atmospheres laboratory. Methanol and ethanol were dried over magnesium methoxide, acetonitrile over calcium hydride. All solvents were stored under nitrogen after distillation. Carbon-13 NMR spectra were recorded with a JEOL JNM-GX400 NMR spectrometer or a Bruker AC200F NMR spectrometer. The compounds [9]aneN$_3$,[5] [9]aneN$_2$S[1] and [9]aneNS$_2$[2–4] were prepared as described previously, [9]aneS$_3$ was purchased from Aldrich Chemical Company and used as received. The compounds [Fe([9]aneS$_3$)$_2$][ClO$_4$]$_2$ and [Fe([9]aneN$_3$)$_2$][ClO$_4$]$_2$ were prepared by previously described methods.[17,20]

CAUTION! although the perchlorate salts described in this work do not appear to be sensitive to shock or heat, these materials, like all perchlorates, should only be prepared in small quantities and treated with caution.

† *Supplementary data available*: the single-crystal absorption spectra of [Fe([9]aneN$_2$S)$_2$][ClO$_4$]$_2$ at room temperature and 10 K. For direct electronic access see http://www.rsc.org/suppdata/dt/1998/2341/, otherwise available from BLDSC (No. SUP 57394, 3 pp.) or the RSC Library. See Instructions for Authors, 1998, Issue 1 (http://www.rsc.org/dalton).
Non-SI units employed: $\mu_B \approx 9.27 \times 10^{-24}$ J T^{-1}, G = 10^{-4} T.

Syntheses

[Fe([9]aneN$_2$S)$_2$][ClO$_4$]$_2$. To a stirred methanol solution (20 cm^3) of iron(II) perchlorate hexahydrate (0.57 g, 1.57 mmol) a methanol solution (5 cm^3) of [9]aneN$_2$S (0.5 g, 3.4 mmol) was added dropwise. The solution was stirred for 0.5 h, during which time a precipitate formed. The product was collected on a filter, washed with methanol and dried under vacuum. Crystallisation from aqueous solution at 4 °C resulted in a crystalline product (yield 0.65 g, 60%) (Found: C, 26.2; H, 5.26; N, 10.2. [C$_{12}$H$_{28}$FeN$_4$S$_2$][ClO$_4$]$_2$ requires C, 26.3; H, 5.16; N, 10.2%). Metathesis with the hexafluorophosphate ion in water produced [Fe([9]aneN$_2$S)$_2$][PF$_6$]$_2$ (Found: C, 22.5; H, 4.60; N, 8.8. [C$_{12}$H$_{28}$FeN$_4$S$_2$][PF$_6$]$_2$ requires C, 22.6; H, 4.42; N, 8.8%). Visible spectrum [λ/nm (ε/M^{-1} cm^{-1}) in CH$_3$CN]: 581 (37), 412 (44). μ_{eff} 2.95 μ_B (300 K). The synthesis and characterisation of this complex has been reported.[21]

[Fe([9]aneN$_2$S)$_2$][ClO$_4$]$_3$. This synthesis was carried out aerobically. An ethanol solution (80 cm^3) of iron(III) perchlorate hexahydrate (1.84 g, 5.2 mmol) was heated at reflux for 0.5 h. To the refluxing solution an ethanol solution (60 cm^3) of [9]aneN$_2$S (1.52 g, 10.4 mmol) was added dropwise over approximately 3 h. The solution was heated under reflux for a further 12 h during which a brown precipitate formed. At the completion of the reflux period the mixture was permitted to cool to room temperature and filtered. The product obtained was filtered, washed with ethanol and dried in air (yield 1.55 g, 40%). The product was recrystallised from concentrated perchloric acid to yield bright orange crystals (Found: C, 22.0; H, 4.29; N, 8.4. [C$_{12}$H$_{24}$FeN$_4$S$_2$][ClO$_4$]$_3$ requires C, 22.3; H, 4.37; N, 8.7%). UV/VIS spectrum: [λ/nm (ε/M^{-1} cm^{-1}) concentrated perchloric acid]: 226 (11 519), 244 (sh), 305 (7073), 450 (250). The compound, when dried, decomposed on standing, but was stable in acidic solution. μ_{eff} 2.3 μ_B (300 K).

[Fe([9]aneNS$_2$)$_2$][ClO$_4$]$_2$. To a stirred solution (20 cm^3) of iron(II) perchlorate hexahydrate (0.57 g, 1.57 mmol) under a nitrogen atmosphere a methanol solution (20 cm^3) of [9]aneNS$_2$ (0.5 g, 3.35 mmol) was added dropwise. Immediately upon commencement of the addition a pale purple precipitate formed. The solution was stirred for a further 0.5 h to ensure complete precipitation. The precipitate was removed by filtration, washed with methanol and dried under vacuum. The product was recrystallised by dissolution in a minimum amount of water, filtered and cooled to 4 °C; brilliant purple crystals formed upon standing (yield 1.26 g, 65%) (Found: C, 24.2; H, 4.49; N, 4.5. [C$_{12}$H$_{26}$FeN$_2$S$_4$][ClO$_4$]$_2$ requires C, 24.8; H, 4.52; N, 4.8%). Metathesis with the hexafluorophosphate ion in water produced [Fe([9]aneNS$_2$)$_2$][PF$_6$]$_2$ (Found: C, 21.5; H, 4.01; N, 4.1. [C$_{12}$H$_{26}$FeN$_2$S$_4$][PF$_6$]$_2$ requires C, 21.4; H, 3.90; N, 4.2). μ_{eff} 0.49 μ_B (300 K). ^{13}C-{^{1}H} NMR (CD$_3$CN): δ 51.03, 50.33, 49.67 (CH$_2$S); 36.56, 36.24, 34.98, 34.87, 34.52, 33.39 (CH$_2$N).

Magnetic studies

Magnetic susceptibility studies were made using a Quantum Design MPMS SQUID magnetometer with an applied field of 1 T. The powdered sample was contained in a calibrated gelatine capsule which was held in the centre of a soda straw fixed to the end of the sample rod. The magnetization values of the instrument were calibrated against a standard palladium sample, supplied by Quantum Design, and also against chemical calibrants such as CuSO$_4$·5H$_2$O and [Ni(en)$_3$][S$_2$O$_3$].

Mössbauer spectroscopy

Mössbauer spectra were measured with a standard electromechanical transducer operating in a symmetrical constant acceleration mode. A conventional helium bath cryostat was employed for temperature control with the sample maintained in exchange gas. Data were collected with an LSI based 1000 channel multichannel analyser. Velocity calibration was made with respect to iron foil. Spectra were fitted with a Lorentzian lineshape.

EPR spectroscopy

The X-(9–10 GHz, TE$_{102}$ rectangular cavity) and Q-band (34 GHz, TE$_{011}$ cylindrical cavity) EPR spectra were measured on a Bruker ESP300E spectrometer. A flow-through cryostat in conjunction with a Eurotherm (B-VT-2000) variable-temperature controller provided temperatures of 120 to 140 K at the sample position in the cavity. Lower temperatures (minimum 2 K) were obtained with a flow-through Oxford instruments ESR910 cryostat in conjunction with an Oxford instruments ITC-4 variable-temperature controller. Spectrometer tuning, signal averaging and subsequent data manipulation were performed with the in-built software (version 3.2). The microwave frequency and magnetic field were calibrated using an EIP 548B microwave frequency counter and a Bruker ER035M gaussmeter, respectively. The *g* matrices were extracted from the EPR spectra of the iron(III) complexes using the SOPHE computer simulation software suite.[22]

Visible spectroscopy

Visible spectra of solutions were recorded with a Hewlett Packard 8450 UV/VIS spectrophotometer. Electronic spectra of single crystals were measured with a modified Cary-17 spectrometer. Low-temperature spectra down to 10 K were obtained using a Leybold Heyaeus ROK 10-300 closed cycle helium cryostat system.

Crystallography

Crystal data and refinement details. [Fe([9]aneN$_2$S)$_2$][ClO$_4$]$_3$, C$_{12}$H$_{28}$Cl$_3$FeN$_4$O$_{12}$S$_2$, M = 646.71. Crystals were orthorhombic, space group *Pmnn*, a = 8.867(2), b = 10.722(1), c = 12.590(2) Å, U = 1197.0(3) Å^3, Z = 2, D_c = 1.794 g cm^3, F(000) = 666, Mo-Kα radiation, λ = 0.710 69 Å, μ = 12.11 cm^{-1}, $R(F_o)$ = 0.056, R' = 0.068, $w = 6.66/\sigma^2F_o + 2.0 \times 10^{-4}\ F_o^2$. [Fe([9]aneNS$_2$)$_2$][ClO$_4$]$_2$, C$_{12}H_{26}Cl_2FeN_2O_8S_4$, M = 581.36. Crystals were monoclinic, space group $P2_1/c$, a = 7.495(2), b = 16.054(4), c = 8.879(3) Å, β = 90.78(3)°, U = 1068.3(5) Å^3, Z = 2, D_c = 1.807 g cm^{-3}, F(000) = 600, Mo-Kα radiation, λ = 0.71 069 Å, μ = 11.90 cm^{-1}, $R(F_o)$ = 0.048, R' = 0.044, $w = 1/\sigma F_o^2$.

For diffractometry the crystals were mounted on glass fibres with cyanoacrylate resin. Lattice parameters at 21 °C were determined by least-squares fits to the setting parameters of 25 independent reflections, measured and refined on an Enraf-Nonius CAD4-F diffractometer with a graphite monochromator. Intensity data were collected in the range $1 < \theta < 25°$. Data were reduced and Lorentz, polarization and numerical absorption corrections were applied using the Enraf-Nonius structure determination package.[23] The structures were solved using the direct methods in SHELX 86[24] and were refined by full-matrix least-squares analysis with SHELX 76.[25] Neutral complex scattering factors were used.[26] Hydrogen atoms were included at calculated sites with fixed isotropic thermal parameters. All non-hydrogen atoms with the exception of disordered atoms were refined anisotropically. Plots were drawn using ORTEP.[27] Listings of bond lengths and angles are given in Tables 1 and 2.

CCDC reference number 186/1017.

Results and Discussion

Syntheses

The mononuclear iron(II) complexes [Fe([9]aneN$_2$S)$_2$]$^{2+}$ and [Fe([9]aneNS$_2$)$_2$]$^{2+}$ were synthesised by adding a methanolic solution of the cyclononane ligands [9]aneN$_2$S and [9]aneNS$_2$,

respectively, to a stirred methanol solution of iron(II) perchlorate. The products formed were recrystallised from water. The syntheses were carried out under an atmosphere of dinitrogen since the solutions of the complexes were air sensitive. Metathesis with ammonium hexafluorophosphate in water produced the hexafluorophosphate salt of the desired iron(II) complex. The synthesis of the $[Fe([9]aneN_2S)_2][ClO_4]_2$ complex has been reported.[21] Synthesis of the mononuclear iron(III) complex $[Fe([9]aneN_2S)_2][ClO_4]_3$ was achieved by the slow addition of an ethanol solution of $[9]aneN_2S$ to a refluxing ethanol solution of iron(III) perchlorate. The brown compound was recrystallised from concentrated perchloric acid to give the desired product which slowly decomposed in air. Attempted synthesis of $[Fe([9]aneNS_2)_2][ClO_4]_3$ by addition of the ligand directly to an iron(III) solution, or by oxidation of the iron(II) analogue, was unsuccessful.

The ^{13}C NMR spectrum of $[Fe([9]aneNS_2)_2]^{2+}$ (CD_3CN) showed a nine line pattern with two groups of resonances, one in the range δ 49–51 assigned to the carbon atom adjacent to the secondary amine, the second at δ 33–37 arising from the carbon atom adjacent to the thioether. The complex potentially can exist in two geometric forms, the *trans*-$[Fe([9]aneNS_2)_2]^{2+}$ isomer with idealised C_{2h} symmetry, expected to exhibit three resonances, and the *cis*-$[Fe([9]aneNS_2)_2]^{2+}$ isomer with molecular symmetry C_2 where each carbon is magnetically inequivalent and hence six resonances are expected. The complexity of the ^{13}C spectrum suggests that both isomers are present in solution. Similar ^{13}C NMR spectra have been observed for the complex $[Co([9]aneN_2S)_2]^{3+}$, and the pure isomers were separated by fractional crystallisation and cation exchange chromatography.[28,29] For $[Fe([9]aneNS_2)_2]^{2+}$ the isomeric forms were not investigated further, although one form preferentially crystallised.

Acidic solutions of $[Fe([9]aneN_2S)_2][ClO_4]_3$ were stable, but basic solutions of the complex rapidly decomposed. This behaviour has been observed for complexes of $[9]aneS_3$ and has been linked to the metal mediated deprotonation and ring opening of the cyclononane to afford vinyl thioether products.[30,31]

Crystal structures

The single-crystal structure of $[Fe([9]aneN_2S)_2][ClO_4]_3$ shows a centrosymmetric cation with the iron atom lying on a 2/*m* symmetry site, with two $[9]aneN_2S$ ligands facially co-ordinating the iron. The complex is conformationally disordered to accommodate this symmetry. A view of the complex cation $[Fe([9]aneN_2S)_2]^{3+}$ with the numbering scheme is shown in Fig. 1 and listings of bond lengths and angles are given in Table 1. The thioether atoms lie in the axial positions with a S–Fe–S angle of 180(1)°. The amine donors in the equatorial positions complete the octahedral co-ordination of the iron(III) ion. The Fe–S bond length [2.272(1) Å] is marginally shorter than that reported for the low-spin iron(III) complex $[Fe([9]aneS_3)_2][ClO_4]_3$ [2.280(3), 2.2846(25), 2.276(3) Å],[19] $[Fe(THT)_2(TPP)]ClO_4$ and $[Fe(PMS)_2(TPP)]ClO_4$ (THT = tetrahydrothiophene, PMS = pentamethylene sulfide and TPP = meso-tetraphenylporphyrin) ($2.336_{ave.}$ and $2.341_{ave.}$ Å, respectively).[32] The Fe–N bond distances are similar to those reported for other low spin Fe–N (amine) systems.[16]

The structure of the iron(II) complex $[Fe([9]aneN_2S)_2][ClO_4]_2$ at 81 K has been reported[21] and was found to crystallise in the monoclinic space group $P2_1/c$ with the Fe atom lying on an inversion centre. At room temperature we found similar cell dimensions ‡ but with the orthorhombic space group *Pmcb*.

‡ Crystal data for $[Fe([9]aneN_2S)_2][ClO_4]_2$, orthorhombic, space group *Pmcb*, $a = 8.094(2)$, $b = 8.6029(7)$, $c = 14.906(3)$ Å; $U = 1037.9(3)$ Å^3, $T = 294$ K, Mo-Kα radiation $\lambda = 0.710\ 69$ Å, $Z = 2$, $D_c = 1.751$ g cm^{-3}, μ(Mo-Kα) = 11.72 cm^{-1}, $R = 0.042$.

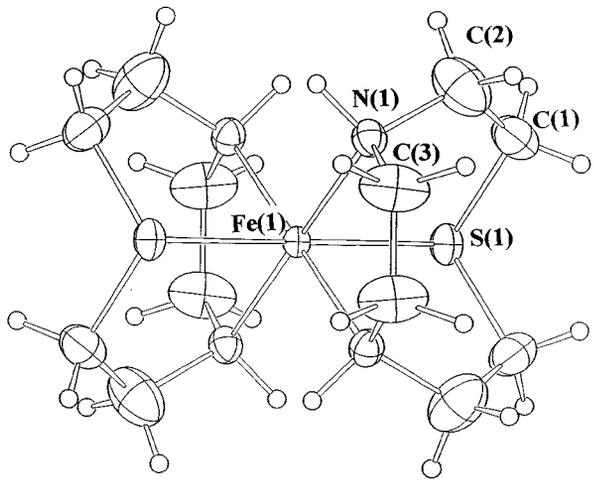

Fig. 1 An ORTEP plot of the complex cation $[Fe([9]aneN_2S)_2]^{3+}$

Table 1 Selected bond lengths (Å) and angles (°) for $[Fe([9]aneN_2S)_2][ClO_4]_3$

S(1)–Fe(1)	2.272(1)	N(1)–Fe(1)	2.006(3)
N(1)–Fe(1)–S(1)	86.6(1)	C(1)–S(1)–Fe(1)	99.4(2)
S(1)–Fe(1)–S(1^{i})	180.0(0)	C(2)–N(1)–Fe(1)	115.7(3)
C(3)–N(1)–Fe(1)	108.4(3)	N(1)–Fe(1)–N(1^{ii})	84.7(2)
N(1)–Fe(1)–N(1^{i})	95.3(2)		

Symmetry operators: i $1 - x$, $1 - y$, $1 - z$. ii x, $1 - y$, $1 - z$.

The iron atom is located on a 2/*m* symmetry site and the complex is necessarily disordered in order to accommodate this symmetry as is the case for the Fe^{III} complex. Presumably cooling to 81 K 'freezes out' this disorder resulting in lower symmetry. Interestingly, the Fe–S and Fe–N bond lengths in the two structures are indistinguishable.

Comparison of the reported structure of $[Fe([9]aneN_2S)_2][ClO_4]_2$ and that determined for $[Fe([9]aneN_2S)_2][ClO_4]_3$ shows a contraction in the Fe–N bond lengths [Fe^{II}, 2.072(2), 2.063(7); Fe^{III} 2.006(3) Å] expected on the basis that the ionic radii decreases from Fe^{II} to Fe^{III}. The contraction in Fe–N bond length was also observed in the analogous complexes $[Fe([9]aneN_3)_2]Cl_2$ and $[Fe([9]aneN_3)_2]Cl_3$ [2.03(1) and 1.99(2) Å, respectively].[33,34] The Fe–S bond distance in $[Fe([9]aneN_2S)_2][ClO_4]_2$ is also longer than that observed for $[Fe([9]aneN_2S)_2][ClO_4]_3$ [Fe^{II}–S 2.337(1) Å, Fe^{III}–S 2.272(1) Å]. However, it has been observed previously that upon reduction of $[Fe([9]aneS_3)_2][ClO_4]_3$ to $[Fe([9]aneS_3)_2][ClO_4]_2$, a contraction of the Fe–S bond lengths [2.280(3), 2.2846(25), 2.276(3) Å to 2.251(1), 2.241(1), 2.259(1) Å, respectively] occurs.[19] Blake *et al.*[19] ascribe this to direct structural evidence for the π-acceptor properties of the thioether donor atoms. They suggest that, as the transition from Fe^{III} to Fe^{II} occurs, π-back bonding increases with the gain of one electron in the t_{2g} orbitals, thereby increasing its contribution to the bond, resulting in a shorter Fe–S bond length. The length of the Fe–S bond of $[Fe([9]aneN_2S)_2][ClO_4]_2$ indicates a high-spin component as it approaches those distances observed in the few known high-spin iron(II) thioether complexes, for example $[Fe([16]aneS_4)I_2]$ [2.475(1) and 2.485(1) Å][35] and [Fe(STPP)Cl] (STPP = 5,10,15,20-tetraphenyl-21-thiaporphyrin) [2.388(3) Å].[36]

The structure of $[Fe([9]aneNS_2)_2][ClO_4]_2$ consists of the cation $[Fe([9]aneNS_2)_2]^{2+}$ and two perchlorate anions. The molecule lies at an inversion centre, with the secondary amines lying *trans* to each other and the thioethers in the equatorial plane of the molecule. An ORTEP drawing of the cation with the numbering scheme is given in Fig. 2, with selected bond distances and angles reported in Table 2. In $[Fe([9]aneNS_2)_2]$-

$[ClO_4]_2$ the Fe–S and Fe–N bond distances are typical of iron(II) in a low-spin configuration. The Fe–S bond distances of 2.249(10) and 2.248(1) Å are similar to those observed in $[Fe([9]aneS_3)_2][ClO_4]_2$ [2.251(1), 2.241(1), 2.259(1) Å].[19] The Fe–N bond distance of 2.038(4) Å is similar to that reported for $[Fe([9]aneN_3)_2]Cl_2$ [2.03(1) Å].[33] The complex $[Fe([18]aneN_2S_4)]^{2+}$ [Fe–N 2.022(4), 2.037(5) Å; Fe–S 2.2578(17), 2.2588(16), 2.2673(16), 2.2674(15) Å] has a similar arrangement of donor atoms and similar bond lengths to those seen in $[Fe([9]aneNS_2)_2]^{2+}$, with the secondary amines located *trans* and the thioether donors located in the equatorial plane.[37]

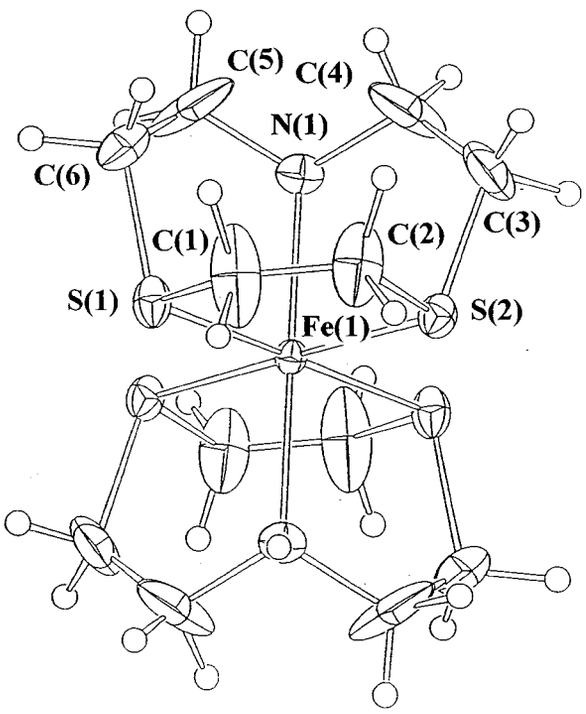

Fig. 2 An ORTEP plot of the complex cation $[Fe([9]aneNS_2)_2]^{2+}$

Table 2 Selected bond lengths (Å) and angles (°) for $[Fe([9]aneNS_2)_2][ClO_4]_2$

S(1)–Fe(1)	2.249(1)	Fe(1)–S(2)	2.248(1)
Fe(1)–N(1)	2.038(4)		
S(1)–Fe(1)–S(1^i)	180.0	S(1)–Fe(1)–S(2)	89.17(5)
S(1)–Fe(1)–S(2^i)	90.83(5)	S(1)–Fe(1)–N(1)	86.3(1)
S(1)–Fe(1)–N(1^i)	93.7(1)	S(2)–Fe(1)–S(2^i)	180.0
S(2)–Fe(1)–N(1)	86.0(1)	S(2)–Fe(1)–N(1^i)	94.0(1)
N(1)–Fe(1)–N(1)	180.0	Fe(1)–S(1)–C(1)	105.1(2)
Fe(1)–S(1)–C(6)	99.0(2)	Fe(1)–N(1)–C(5)	112.6(4)
Fe(1)–S(2)–C(2)	105.3(2)	Fe(1)–S(2)–C(3)	98.1(2)
Fe(1)–N(1)–C(4)	115.4(3)		

Symmetry operator: i $-x, -y, -z$.

Mössbauer spectroscopy

Mössbauer spectra of $[Fe([9]aneN_2S)_2][ClO_4]_2$, $[Fe([9]aneNS_2)_2][ClO_4]_2$ and $[Fe([9]aneN_2S)_2][ClO_4]_3$ were measured in the absence of an applied magnetic field. The isomer shift (δ) and quadrupole splitting (ΔE_Q) for the $[Fe([9]aneN_{3-x}S_x)_2]^{n+}$ ($x = 3$–0; $n = 2$ or 3) series are reported in Table 3. In order to estimate the isomer shift for $[Fe([9]aneN_3)_2][ClO_4]_2$ (0.6 mm s^{-1}) the Mössbauer parameters for an analogous low-spin Fe^{II} complex $[Fe([14]aneN_4)(CH_3CN)_2][PF_6]_2$ were employed.[38] Analysis of the change in isomer shift for the series of iron(II) complexes suggested that as the number of thioether donor atoms increased the isomer shift decreased. The observed decrease in δ may be explained on the basis of the π-acceptor properties of the thioether donor, the π-acceptance decreasing the d electron shielding of the s electrons around the nucleus. No correlation between the quadrupole splitting and the donor set in the same iron(II) series was observed. The effect on the quadrupole splitting of the equatorial and axial donor groups has been investigated for a series of low-spin iron(II) complexes of general formula *trans*-FeA_2B_4.[39] A decrease in ΔE_Q was observed when B was a better π-acceptor than A, the axial ligand. A similar decrease is observed for the complexes $[Fe([9]aneN_2S)_2][ClO_4]_2$ and $[Fe([9]aneNS_2)_2][ClO_4]_2$ (0.57 and 0.28 mm s^{-1}, respectively). Small lattice contributions to ΔE_Q were excluded by the exclusive use of perchlorate salts.[38]

The magnitude of the isomer shift for the iron(III) complex $[Fe([9]aneN_2S)_2]^{3+}$ (0.25 mm s^{-1}) is within the range reported for low-spin iron(III) complexes. As expected, the isomer shift for the iron(III) complex is smaller than that measured for the iron(II) analogue $[Fe([9]aneN_2S)_2][ClO_4]_2$, based on the relative isomer shifts observed for the complexes $[Fe([9]aneS_3)_2]^{3+}$ (0.20 mm s^{-1}) and $[Fe([9]aneS_3)_2]^{2+}$ (0.35 mm s^{-1}).[18] Whilst the isomer shift for $[Fe([9]aneN_3)_2]Cl_3\cdot 5H_20$ (−0.02 mm s^{-1}) [18] is lower than that for the thioether analogues, no correlation between the number of thioether donors and the isomer shift is apparent. Similarly, there appears to be no correlation between the number of thioether donors and the quadrupole splitting for the iron(III) complexes. The large ΔE_Q for $[Fe([9]aneN_2S)_2]^{3+}$ (2.72 mm s^{-1}) is comparable to that observed for $[Fe([9]aneS_3)_2]^{3+}$ (2.02 mm s^{-1}) and may be ascribed to the tetragonal distortion of the complex.

Magnetic susceptibility

The magnetic susceptibility for a ground solid sample of $[Fe([9]aneNS_2)_2][ClO_4]_2$ showed the typical temperature independent susceptibility behaviour for a spin-paired complex possessing a $^1A_1$ ground state.[40] The magnetic moment at 300 K was 0.49 μ_B decreasing to 0.08 μ_B at 2 K.

Variable-temperature susceptibility measurements on a solid ground sample of $[Fe([9]aneN_2S)_2][ClO_4]_2$ in the range 2–300 K exhibited a temperature-dependent magnetic moment. Between 4.2 and 150 K a magnetic moment of 0.5 μ_B was observed, and this gradually increased to 2.95 μ_B at 300 K. The spin-only

Table 3 Isomer shifts (δ) and quadrupole splittings (ΔE_Q) of iron(II) and iron(III) complexes of $[9]aneN_{3-x}S_x$ ($x = 3$–0) ligands

	T/K	δ[a]/mm s^{-1}	ΔE_Q/mm s^{-1}	Spin state, S
$[Fe([9]aneS_3)_2]^{2+}$ [b]	4.2	0.35	0.33	0
	77	0.34	0.33	
	293	0.27	0.32	
$[Fe([9]aneNS_2)_2]^{2+}$	4.2	0.43	0.28	0
$[Fe([9]aneN_2S)_2]^{2+}$	4.2	0.52	0.57	0
	293	0.50	0.45	Intermediate spin
$[Fe([9]aneS_3)_2]^{3+}$ [b]	4.2	0.20	2.02	$\frac{1}{2}$
	293	0.11	1.91	
$[Fe([9]aneN_2S)_2]^{3+}$	4.2	0.25	2.72	$\frac{1}{2}$
$[Fe([9]aneN_3)_2]^{3+}$ [b]	298	−0.02	0.98	$\frac{1}{2}$

[a] ±0.01 mm s^{-1}, relative to α-Fe. [b] Ref. 18.

magnetic moment for the high-spin d^6 configuration is 4.90 μ_B whilst the low-spin state is diamagnetic.[40] The temperature dependent behaviour of the magnetic susceptibility displayed by this complex is typical of a thermally induced high-spin (HS) $\rightleftharpoons$ low-spin (LS) transition between the high-spin $^5T_{2g}$ ($t_{2g}^4e_g^2$) and low-spin $^1A_{1g}$ (t_{2g}^6) ground states.[41] The magnitude of the magnetic moment at 300 K indicates that the spin-state transformation is not complete at this temperature.

The solution magnetic susceptibility of $[Fe([9]aneN_2S)_2]^{2+}$ also exhibited a temperature dependence. Given that the two spin states are derived from a singlet $^1A_{1g}$ and a quintet $^5T_{2g}$ ground state, the equilibrium constant K_{eq} for the process, $[Fe([9]aneN_2S)_2]^{2+}$ (t_{2g}^6) $\rightleftharpoons$ $[Fe([9]aneN_2S)_2]^{2+}$ ($t_{2g}^4e_g^2$) is given by equation (1), where m = mole fraction of the spin isomer,

$$K_{eq} = \frac{m_{hs}}{m_{ls}} = \frac{(\mu^2_{exptl} - \mu^2_{ls})}{(\mu^2_{hs} - \mu^2_{exptl})} \quad (1)$$

μ_{ls} and μ_{hs} represent the magnetic moments for the low-spin and the high-spin isomer, respectively. The values for the high- and low-spin moments are taken from the spin-only values, 4.90 and 0 μ_B, respectively,[40] although the precise magnitude of the high-spin magnetic moment depends on effects such as the spin–orbit coupling, electron Zeeman effects and low symmetry distortions, and values employed previously range from 5.5 to 4.9 μ_B.[14,42] Assuming values for μ_{hs} of both 4.9 and 5.5 μ_B, the thermodynamic parameters (ΔH^0 20–22 kJ mol^{-1}; ΔS^0 53–60 J mol^{-1} K^{-1}) calculated from plots of $\ln K_{eq}$ *versus* $1/T$ are similar to other values reported for analogous thermally induced high-spin $\rightleftharpoons$ low-spin transitions in Fe^{II} complexes.[43,44] The dominant enthalpic term is provided by inner-sphere reorganisation, such as the change in metal–ligand bond length[45,46] exhibited in $[Fe([9]aneN_2S)_2][ClO_4]_2$ compared to the low-spin complexes $[Fe([9]aneNS_2)_2][ClO_4]_2$ and $[Fe([9]aneS_3)_2][ClO_4]_2$.

The magnetic susceptibility for $[Fe([9]aneN_2S)_2][ClO_4]_3$ (4.2–300 K) follows the Curie–Weiss law in the region 300 K (2.3 μ_B) to 4.2 K (1.9 μ_B). The higher than spin-only value for the magnetic moment for iron(III) (300 K, 1.73 μ_B) arises from an orbital contribution associated with the degenerate $^2T_{2g}$ ground state, although the combination of spin–orbit and low symmetry splitting will quench this to some extent. The measure of the axial splitting is detailed in the analysis of the EPR spectra, see below. Using the g matrix obtained from the EPR investigation, the magnetic susceptibility data were fit to a simple model ($\mathscr{H} = -\lambda L\cdot S + \mu L_z$) to estimate the spin–orbit coupling parameter, λ, and the axial ligand-field parameter, μ. Maintaining μ/λ as -2.915, determined from the EPR analysis, the magnetic susceptibility data can be fit using a value of $\lambda = -260 \pm 10$ cm^{-1}, with $\mu \approx 760$ cm^{-1}.[40,47] The low-spin d^5 configuration has been observed previously for iron(III) amine complexes such as $[Fe(N_6sar)]Cl_3\cdot H_2O$ [2.55 μ_B (295 K); $\lambda = -300 \pm 50$ cm^{-1}; $\mu = 400 \pm 100$ cm^{-1}],[16] $[Fe([9]aneN_3)_2]Br_3\cdot 5H_2O$ [2.3 μ_B (295 K)],[20] $[Fe(dtne)]Br_3\cdot 3H_2O$ [dtne = 1,2-bis(1,4,7-triazacyclonon-1-yl)ethane] [2.7 μ_B (293 K)],[48] and $[Fe(diammac)]^{3+}$ (diammac = 6,13-dimethyl-1,4,8,11-tetraazacyclotetradecane-6,13-diamine) [2.20 μ_B (295 K); $\lambda = -310$ cm^{-1}; $\mu = 940$ cm^{-1}].[49]

EPR spectroscopy

The anisotropic frozen solution EPR spectra of $[Fe([9]aneN_2S)_2]^{3+}$ are typical of a low spin d^5 ($S = \frac{1}{2}$) electron configuration in a distorted octahedral field (Fig. 3). The solid-state X-band spectrum of $[Fe([9]aneN_2S)_2]^{3+}$ reveals an axially symmetric low-spin iron(III) ion, with $g_\perp = 2.607$ and $g_\parallel = 1.599$. At Q-band frequencies the perpendicular resonance is resolved into two components, characteristic of a rhombically distorted low-spin iron(III) centre. Computer simulation of this spectrum yielded the g values $g_x = 2.687$, $g_y = 2.526$ and $g_z = 1.599$. The

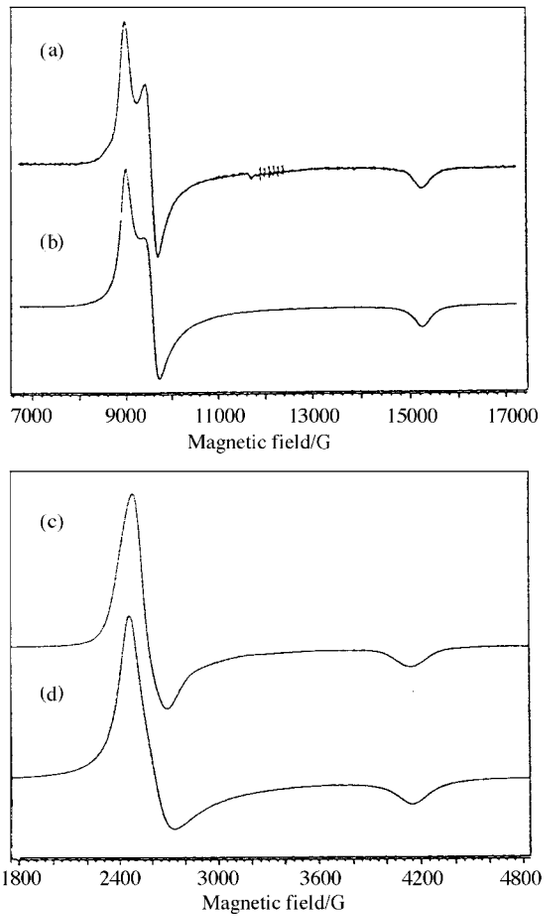

Fig. 3 Multifrequency EPR spectra of $[Fe([9]aneN_2S)_2]^{3+}$. (a) Q-band solid-state spectrum, $\nu = 33.935\ 70$ GHz, $T = 120$ K (the six resonances around $g = 2$ arise from Mn^{II} in the Suprasil quartz EPR tubes); (b) SOPHE computer simulation of (a); (c) X-band solid-state spectrum, $\nu = 9.298\ 261$ GHz, $T = 120$ K; (d) SOPHE computer simulation of (c)

difference in g_z values obtained from the X- and Q-band spectra arises from the non-linearity of the magnetic field at high fields ≈ 16 000 gauss. Thus the estimate of g_z from the X-band spectrum is more reliable. Resolution of the g_x and g_y resonances in the solid-state Q-band spectrum reveals a greater insight into the actual symmetry and hence a more accurate analysis of the spectrum from this complex is possible. The degree of rhombicity is best judged by the absolute value of R/μ, where μ and R are the axial and rhombic distortions, respectively, as this avoids the approximation of a spin–orbit coupling parameter. The three g values from the simulation were analysed to determine the values of μ and R, employing methods reported previously.[50] For $[Fe([9]aneN_2S)_2][ClO_4]_3$ $|R/\mu| = 0.197$ demonstrating the rhombic distortion the [9]ane-N_2S ligand places on the iron(III) ion.

The similarity of the g values for $[Fe([9]aneN_2S)_2]^{3+}$ in the solid state and solution ($g_x = 2.758$, $g_y = 2.516$ and $g_z = 1.580$) indicates that the geometry around the iron(III) centre is similar in both states and the complex retains its integrity upon dissolution in acidic solution. The slight differences in the g values are attributed to the symmetry distortion of crystal packing forces present only in the solid state.

It has been reported that no EPR spectrum was observed for the complex $[Fe([9]aneN_3)_2]^{3+}$ between 100–295 K, an observation attributed to the fast spin–lattice relaxation times of low-spin iron(III).[51] Analysis of the EPR spectrum (X-band) of $[Fe([9]aneS_3)_2]^{3+}$ at 77 K resulted in the determination of $g_\perp = 2.328$ and $g_\parallel = 1.942$.[30] The observation of the low-spin iron(III) signal for $[Fe([9]aneS_3)_2]^{3+}$ and $[Fe([9]aneN_2S)_2]^{3+}$ and not $[Fe([9]aneN_3)_2]^{3+}$ is probably due to the deviation of the former two complexes from octahedral symmetry which

decreases the electron spin–lattice relaxation time due to a greater energy separation of the ground and nearby excited states, Orbach relaxation.[52] An EPR spectrum of $[Fe([9]aneS_3)_2]^{3+}$ was also measured at Q-band frequencies to determine if the complex was indeed axial or if it was rhombically distorted, with the separation of the perpendicular resonance into its component g_x and g_y values not being resolved at X-band frequencies. No resolvable splitting of the perpendicular resonance was observed, indicating that if a rhombic distortion exists in the complex $[Fe([9]aneS_3)_2]^{3+}$ it is smaller than the line width of the perpendicular resonance. The crystal structure of $[Fe([9]aneS_3)_2]^{3+}$ reveals two axially elongated Fe–S bond distances.[19] The distortion of the $[9]aneS_3$ ligand on the iron(III) centre is only in the z axis with the x and y axes equivalent. This is in contrast to the $[9]aneN_2S$ ligand which places a rhombic distortion on the x, y and z axes.

Electronic spectroscopy

The electronic spectra of $[Fe([9]aneN_2S)_2]^{2+}$, $[Fe([9]aneNS_2)_2]^{2+}$ and $[Fe([9]aneN_2S)_2]^{3+}$ were investigated in solution and as single crystals. The visible spectra of the first two complexes appear typical of octahedral low-spin iron(II), with d–d bands corresponding to the $^1A_{1g} \longrightarrow {}^1T_{1g}$ and $^1A_{1g} \longrightarrow {}^1T_{2g}$ spin-allowed transitions or their low-symmetry split components. The band positions at room temperature (solution spectra) and 10 K (single crystal spectra) are given in Table 4. Solution data for $[Fe([9]aneN_3)_2]^{2+}$ and $[Fe([9]aneS_3)_2]^{2+}$ complexes are also included. An increase in $10Dq$ is observed from N_6 to S_6 co-ordination demonstrating that for low-spin iron(II) the thioether donors exert a stronger ligand field than amine donors, a point which has been previously noted in the literature.[11,18] The 1700 cm^{-1} difference in $10Dq$ from N_6 to S_6 co-ordination is similar to that found for the analogous cobalt(III) complexes.[11] The nephelauxetic parameter, $\beta = B_{complex}/B_{free\ ion}$ decreases markedly with the number of thioether donors from 0.54 (N_6) to 0.36 (S_6) reflecting the high degree of covalency in the iron(II)–thioether bond. The value of β for $[Fe([9]aneS_3)_2]^{2+}$ (0.36) is lower than that reported for $[Fe(CN)_6]^{4-}$ (0.49) where the metal–ligand bond also has a large degree of π-acceptor character.[53]

The single-crystal absorption spectra of $[Fe([9]aneN_2S)_2][ClO_4]_2$ at room temperature and 10 K exhibits three bands at 16 650, 20 550 and 25 250 cm^{-1} (SUP 57394). It is tempting to assign the two lowest energy bands to pseudo-tetragonal splitting of the $^1T_{1g}$ state into $^1A_2$ and ^1E components and the band at 25 250 cm^{-1} to the unsplit $^1A_{1g} \longrightarrow {}^1T_{2g}$ transition. Since the $^1A_1 \longrightarrow {}^1A_2$ transition depends only on the in-plane ligand field strength, in this case that of the amine donors, it is expected to lie at approximately the same energy as the parent octahedral $^1A_{1g} \longrightarrow {}^1T_{1g}$ transition in $[Fe([9]aneN_3)_2]^{2+}$ which indeed it does. Within the simple angular overlap model,[54] the apparent 3900 cm^{-1} splitting of the $^1T_{1g}$ state, assuming the higher energy component is assigned to the $^1A_1 \longrightarrow {}^1E$ transition, is given by equation (2) where xy and z denote the equatorial and axial donors, respectively. On the basis that $e_\sigma(S) \approx e_\sigma(N)$, an assumption which holds well for Co^{III} complexes,[10,11] the above expression results in an unrealistic value of $e_\pi(S) \approx -2000$ cm^{-1}. Furthermore, the energy difference of $10Dq(z) - 10Dq(xy) = 7800$ cm^{-1} indicates that the axial thioether donors exert a much stronger ligand field than the equatorial amine donors and this is not consistent with the $10Dq$ values for the $[9]aneS_6$ and $[9]aneN_6$ complexes of iron(II) reported in Table 4 which differ by only 1700 cm^{-1}. Also, the Fe^{II}–S bonds in $[Fe([9]aneN_2S)_2]^{2+}$ are approximately 0.07 Å longer compared to those in $[Fe([9]aneS_3)_2]^{2+}$ and accordingly one would have expected a significant reduction in $Dq(z)$ in the former complex, not an increase. In fact, the 3900 cm^{-1} splitting is similar to that reported for $[Fe([14]aneN_4)(CN)_2]$[55] and it seems very unlikely that the axial thioether donors could exert a ligand field strength comparable to CN^-. Consequently, we feel that assignment of the band at 20 550 cm^{-1} to the $^1A_1 \longrightarrow {}^1E$ transition arising from the tetragonal splitting of the $^1T_{1g}$ state is not credible and therefore an alternative assignment is sought. On this matter, we have previously observed weak, low-lying $\pi(S) \longrightarrow Fe^{II}$ ligand-to-metal charge-transfer transitions in Ni^{II} complexes involving thioether donors between 22 000 and 26 000 cm^{-1}.[56] The fact that such a transition has moved to even lower energy (20 550 cm^{-1}) in $[Fe([9]aneN_2S)_2]^{2+}$ is not too surprising given the rather long Fe^{II}–S bond distances in this complex.

$$\Delta(^1T_{1g}) = -3/2\,[e_\sigma(xy) - e_\sigma(z)] + 2\,[e_\pi(xy) - e_\pi(z)] \equiv -\tfrac{1}{2}\,[10Dq(xy) - 10Dq(z)] \quad (2)$$

In the spectra of $[Fe([9]aneN_2S)_2][ClO_4]_2$ an additional lower energy band is observed at approximately 9500 cm^{-1} which exhibits pronounced temperature dependence (Fig. 4). The band is assigned to the $^5T_{2g} \longrightarrow {}^5E_g$ transition associated with the analogous high-spin Fe^{II} complex. The temperature dependence is attributed to a high-spin/low-spin thermal equilibrium and can be analysed using the Boltzmann distribution equation (3), where I_0 is the intensity at T_0, the temperature

$$I_T = I_0 \frac{e^{(-E/0.695\,08kT)}}{e^{(-E/0.695\,08T_0)}} \quad (3)$$

where there is no absorbance of the high-spin component, and I is the absorbance at temperature, T. Using this expression, the energy separation, E, of the high-spin, $^5T_{2g}$, and low-spin,

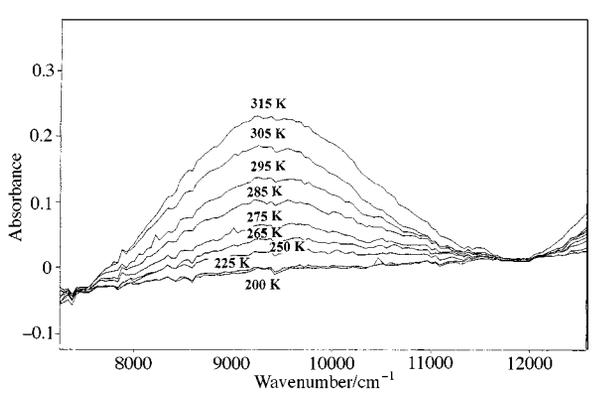

Fig. 4 Temperature dependence of the 9500 cm^1 band in the single-crystal absorption spectra of $[Fe([9]aneN_2S)_2][ClO_4]_2$

Table 4 Spectroscopic data[a] for $[Fe([9]aneN_xS_{3-x})_2]^{2+}$ (x = 3–0)

Complex	Medium[b]	$^1A_{1g} \longrightarrow {}^1T_{1g}$	$^1A_{1g} \longrightarrow {}^1T_{2g}$	$10Dq$	B	β
$[Fe([9]aneN_3)_2]^{2+}$	Solution	16 650(6)	25 850(17)	18 950	575	0.54
$[Fe([9]aneN_2S)_2]^{2+}$	Solution	17 200(56)	24 650(36)			
	Crystal	16 650, 20 550[c]	25 250			
$[Fe([9]aneNS_2)_2]^{2+}$	Solution	18 150(37)	24 250(44)			
	Crystal	18 400	23 700,[c] 26 950			
$[Fe([9]aneS_3)_2]^{2+}$	Solution	19 150(53)	25 300(52)	20 690	385	0.36

[a] Transition energies, $10Dq$ and B all in cm^{-1}. [b] Solution spectra measured at room temperature, crystal spectra at ≈10 K. [c] These bands may not arise from d–d bands (see text).

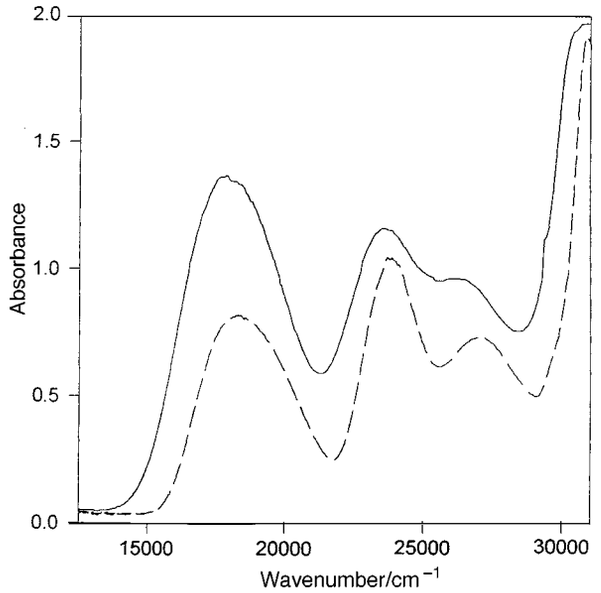

Fig. 5 The single-crystal absorption spectra of $[Fe([9]aneNS_2)_2][ClO_4]_2$ at room temperature (——) and 10 K (– – –)

$^1A_{1g}$, ground states is calculated at approximately 1700 cm^{-1}, consistent with temperature dependence observed for the magnetic susceptibility. For high-spin iron(II) complexes, the $^5T_{2g} \longrightarrow {}^5E_g$ transition corresponds directly to $10Dq$. The smaller value of 9500 cm^{-1} for $10Dq$ compared to the low-spin complex where $10Dq = 17\,200$ cm^{-1}, is a result of the longer metal–ligand bonds arising from the occupation of the antibonding e_g orbitals in the ground state of the high-spin complex. Although the ^5E_g excited state is Jahn–Teller active, tetragonal splitting of this band is not observed.

The single-crystal absorption spectra of $[Fe([9]aneNS_2)_2][ClO_4]_2$ at room temperature and 10 K are shown in Fig. 5. The splitting of the lower energy $^1A_{1g} \longrightarrow {}^1T_{1g}$ transition is not resolved but the low-temperature band is distinctly asymmetric. At first glance, it appears that a prominent low-symmetry splitting of approximately 3000 cm^{-1} occurs for the higher lying $^1A_{1g} \longrightarrow {}^1T_{2g}$ transition but, once again, the magnitude of this splitting is unrealistic given the similar $10Dq$ values for the $[9]aneN_3$ and $[9]aneS_3$ ligands, and therefore we turn to the possibility of one of the components being due to a weak, low-lying $\pi(S) \longrightarrow Fe^{II}$ ligand-to-metal charge-transfer transition. Of the two components, only the higher energy band at 26 950 cm^{-1} leads to an acceptable value for the Racah B parameter and therefore is assigned to the $^1A_{1g} \longrightarrow {}^1T_{2g}$ transition. The shift of the $\pi(S) \longrightarrow Fe^{II}$ charge-transfer transition over 3000 cm^{-1} to higher energy compared to $[Fe([9]aneN_2S)_2]^{2+}$ is not unreasonable given the 0.07 Å shorter Fe^{II}–S bond distances present in the $[Fe([9]aneNS_2)_2]^{2+}$ complex.

The electronic spectra of low-spin iron(III) complexes have not been extensively investigated. In addition, the spectra are complicated by the presence of intense, low-lying ligand-to-metal charge-transfer transitions which partially obscure the d–d transitions. Low-spin iron(III) in octahedral symmetry has a $^2T_{2g}$ ground state with lower-lying transitions to $^4T_{1g}$, $^4T_{2g}$, $^2A_{2g}$, $^2T_{1g}$ and ^2E_g excited states possible in that order. The single-crystal absorption spectrum of $[Fe([9]aneN_2S)_2][ClO_4]_3$ exhibits bands at approximately 20 000, 21 500 and 23 000 cm^{-1} and are tentatively assigned as spin-allowed d–d transitions to the $^2A_{2g}$, $^2T_{1g}$ and ^2E_g excited states, respectively. These assignments do not take into account any tetragonal splitting of the octahedral states but nonetheless are consistent with those previously reported for the low-spin iron(III) complexes $[Fe(diammac)]^{3+}$ and $[Fe([9]aneS_3)_2]^{3+}$.[49,18] The solution spectrum also exhibits intense bands at approximately 32 800 (7070 м$^{-1}$ cm^{-1}) and 44 250 cm^{-1} (11 519 м$^{-1}$ cm^{-1}), presumably due to $S \longrightarrow Fe^{III}$ and $N \longrightarrow Fe^{III}$ ligand-to-metal charge-transfer transitions, respectively.

References

1 L. R. Gahan, G. A. Lawrance and A. M. Sargeson, *Aust. J. Chem.*, 1982, **35**, 1119.
2 D. Parker, A. S. Craig, G. Ferguson and A. J. Lough, *Polyhedron*, 1989, **8**, 2951.
3 A. S. Craig, R. Kataky, R. C. Matthews, D. Parker, G. Ferguson, A. Lough, H. Adams, N. Bailey and H. Schneider, *J. Chem. Soc., Perkin Trans. 2*, 1990, 1523.
4 A. McAuley and S. Subramanian, *Inorg. Chem.*, 1990, **29**, 2830.
5 K. Wieghardt, W. Schmidt, B. Nuber and J. Weiss, *Chem. Ber.*, 1979, **112**, 2220.
6 S. R. Cooper, *Acc. Chem. Res.*, 1988, **21**, 141.
7 I. I. Creaser, J. M. Harrowfield, A. J. Herlt, A. M. Sargeson, J. Springborg, R. J. Geue and M. R. Snow, *J. Am. Chem. Soc.*, 1977, **99**, 3181.
8 L. R. Gahan, T. W. Hambley, A. M. Sargeson and M. R. Snow, *Inorg. Chem.*, 1982, **21**, 2699.
9 P. Osvath, A. M. Sargeson, B. W. Skelton and A. H. White, *J. Chem. Soc., Chem. Commun.*, 1991, 1036.
10 T. M. Donlevy, L. R. Gahan, T. W. Hambley and R. Stranger, *Inorg. Chem.*, 1992, **21**, 4376.
11 J. I. Bruce, L. R. Gahan, T. W. Hambley and R. Stranger, *Inorg. Chem.*, 1993, **32**, 5997.
12 I. I. Creaser, A. M. Sargeson and A. Zanella, *Inorg. Chem.*, 1983, **22**, 4022.
13 T. M. Donlevy, L. R. Gahan and T. W. Hambley, *Inorg. Chem.*, 1994, **33**, 2668.
14 L. L. Martin, K. S. Hagen, A. Hauser, R. L. Martin and A. M. Sargeson, *J. Chem. Soc., Chem. Commun.*, 1988, 1313.
15 I. I. Creaser, L. M. Engelhardt, J. M. Harrowfield, A. M. Sargeson, B. W. Skelton and A. H. White, *Aust. J. Chem.*, 1993, **46**, 465; P. A. Anderson, I. I. Creaser, C. Dean, E. Horn, L. L. Martin, A. M. Sargeson, M. R. Snow and E. R. T. Tiekink, *Aust. J. Chem.*, 1993, **46**, 449.
16 L. L. Martin, R. L. Martin, K. S. Murray and A. M. Sargeson, *Inorg. Chem.*, 1990, **29**, 1387.
17 K. Wieghardt, H.-J. Küppers and J. Weiss, *Inorg. Chem.*, 1985, **24**, 3067.
18 H.-J. Küppers, K. Wieghardt, B. Nuber, J. Weiss, E. Bill and A. X. Trautwein, *Inorg. Chem.*, 1987, **26**, 3762.
19 A. J. Blake, A. J. Holder, T. I. Hyde and M. Schröder, *J. Chem. Soc., Chem. Commun.*, 1989, 1433.
20 K. Wieghardt, W. Schmidt, W. Herrmann and H.-J. Küppers, *Inorg. Chem.*, 1983, **22**, 2953.
21 U. Heinzel, A. Henke and R. Mattes, *J. Chem. Soc., Dalton Trans.*, 1997, 501.
22 D. Wang and G. R. Hanson, *J. Magn. Reson.*, 1995, **117**, 1; D. Wang and G. R. Hanson, *Appl. Magn. Reson.*, 1996, **11**, 401.
23 Enraf-Nonius Structure Determination Package, Enraf-Nonius, Delft, 1985.
24 G. M. Sheldrick, SHELXS 86, in *Crystallographic Computing 3*; eds. G. M. Sheldrick, C. Krüger and R. Goddard, Oxford University Press, Oxford, 1985, pp. 175–189.
25 G. M. Sheldrick, SHELX 76, Program for Crystal Structure Determination, University of Cambridge, 1976.
26 D. T. Cromer and J. T. Waber, *International Tables for X-Ray Crystallography*, Kynoch Press, Birmingham, 1974, vol. 4.
27 C. K. Johnson, ORTEP, A Thermal Ellipsoid Plotting Program, Oak Ridge National Laboratory, Oak Ridge, TN, 1965.
28 T. W. Hambley and L. R. Gahan, *Acta Crystallogr., Sect. C*, 1986, **42**, 1322.
29 L. R. Gahan, T. W. Hambley, G. H. Searle, M. J. Bjerrum and E. Larsen, *Inorg. Chim. Acta*, 1988, **147**, 17.
30 M. N. Bell, A. J. Blake, A. J. Holder, T. I. Hyde and M. Schröder, *J. Chem. Soc., Dalton Trans.*, 1990, 3841.
31 A. J. Blake, A. J. Holder, T. I. Hyde, H.-J. Küppers, M. Schröder, S. Stötzel and K. Wieghardt, *J. Chem. Soc., Chem. Commun.*, 1989, 1600.
32 T. Mashiko, C. A. Reed, K. J. Haller, M. E. Kastner and W. R. Scheidt, *J. Am. Chem. Soc.*, 1981, **103**, 5758.
33 J. C. A. Boeynes, A. G. S. Forbes, R. D. Hancock and K. Wieghardt, *Inorg. Chem.*, 1985, **24**, 2926.
34 R. E. Marsh, *Acta Crystallogr., Sect. B*, 1987, **43**, 174.
35 D. L. Hughes, M. Jimenez-Tenorio, G. J. Leigh, A. Houlton and J. Silver, *J. Chem. Soc., Dalton Trans.*, 1992, 2033.
36 L. Latos-Grażyński, J. Lisowski, M. M. Olmstead and A. L. Balch, *Inorg. Chem.*, 1989, **28**, 1183.

37 G. Reid and M. Schröder, *Chem. Soc. Rev.*, 1990, **19**, 239.
38 J. C. Dabrowiak, P. H. Merrell, J. A. Stone and D. H. Busch, *J. Am. Chem. Soc.*, 1973, **95**, 6613.
39 G. M. Bancroft, M. J. Mays and B. E. Prater, *J. Chem. Soc. A*, 1970, 956.
40 B. N. Figgis, *Introduction to Ligand Fields*, Wiley Interscience, New York, 1966.
41 M. Bacci, *Coord. Chem. Rev.*, 1988, **86**, 245.
42 E. V. Dose, K. M. M. Murphy and L. J. Wilson, *Inorg. Chem.*, 1976, **15**, 2622.
43 H. Toftlund, *Coord. Chem. Rev.*, 1989, **94**, 67.
44 E. König, *Struct. Bonding* (*Berlin*), 1991, **76**, 51.
45 K. A. Reeder, E. V. Dose and L. J. Wilson, *Inorg. Chem.*, 1978, **17**, 1071.
46 E. König and K. J. Watson, *Chem. Phys. Lett.*, 1970, **6**, 457.
47 G. A. Webb, *Coord. Chem. Rev.*, 1969, **4**, 107.
48 K. Wieghardt, I. Tolksdorf and W. Herrmann, *Inorg. Chem.*, 1985, **24**, 1230.
49 P. V. Bernhardt, P. Comba, T. W. Hambley and G. A. Lawrance, *Inorg. Chem.*, 1991, **30**, 942.
50 T. L. Bohan, *J. Magn. Reson.*, 1977, **26**, 109.
51 K. Pohl, K. Wieghardt, W. Kaim and S. Steenken, *Inorg. Chem.*, 1988, **27**, 440.
52 R. Orbach, *Proc. R. Soc. London A*, 1961, **264**, 458; R. Orbach, *Proc. R. Soc. London A*, 1961, **264**, 485.
53 A. P. B. Lever, *Inorganic Electronic Spectroscopy*, Elsevier, Amsterdam, 2nd edn., 1984.
54 D. A. Cruse, J. E. Davies, M. Gerloch, J. H. Harding, D. J. Mackey and R. F. McMeeking, CAMMAG – a FORTRAN Computer Package, University Chemical Laboratory, Cambridge, 1979.
55 D. D. Watkins, jun., D. P. Riley, J. A. Stone and D. H. Busch, *Inorg. Chem.*, 1976, **15**, 387.
56 W. Shore and R. Stranger, unpublished work.

Received 19*th February* 1998; *Paper* 8/01417E